

Numerical simulation of HPT processing

P Verleysen¹, F Van den Abeele² and J Degrieck¹

¹ Department of Materials Science and Engineering, Ghent University, Ghent, Belgium

² Vikar R&D, Aalter, Belgium

E-mail: Patricia.Verleysen@UGent.be

Abstract. The principle of achieving high strength and superior properties in metal alloys through the application of severe plastic deformation has been exploited in the metal processing industry for many decades. In this contribution finite element simulations are presented of the HPT process. As opposed to most studies in literature, in which rigid sample holders are considered, the real elasto-plastic behavior of the holders is modeled. The simulations show that during the compression stage, plastic deformation occurs in the holders: initially, at the outside boundary of the sample cavity and, at a later stage, underneath the centre of the sample. The latter region of plastic deformation is rapidly growing and has a non-negligible effect on the response of the sample. Major conclusion is that the sample holders, and more specific, their deformability is key for the conditions in the specimen. Indeed, it severely affects important parameters for both the microstructural changes in the sample material, such as the amplitude and distribution of the hydrostatic stress, and its final shape.

1. Introduction

Nanocrystalline materials (NCM) represent a whole generation of solids with new atomic structures and properties by utilizing the atomic arrangements in the cores of defects such as grain boundaries, interphase boundaries or dislocations. Severe plastic deformation (SPD) achieves very fine crystals by the use of severe straining and deforming the material under high pressure to prevent the material from failing. SPD processing is defined in [1] as any method of metal forming under an extensive hydrostatic pressure that may be used to impart a very high strain to a bulk solid without the introduction of any significant change in the overall dimensions of the sample and having the ability to produce exceptional grain refinement. The most important methods to achieve SPD are Equal Channel Angular Pressing (ECAP) and High Pressure Torsion (HPT). On a laboratory scale, the HPT process is one of the most promising techniques. It imposes very high shear strains to a heavily compressed bulk solid without introducing a significant change in sample dimensions [1].

A HPT sample has a disk shape, with a height around 1mm and a diameter between 10 and 20mm. The sample is compressed between two anvils with a pressure that varies from 1GPa up to 10GPa. Once the pressure is applied, one anvil is rotated with respect to the other. Due to friction in contact surfaces between the specimen and the anvils, the specimen is deformed by shear force. The main volume of the specimen is strained under hydrostatic compression because of the applied pressure and the pressure of the outer layers of the sample. Two distinct types of high pressure torsion exist, each with its own features. The first type, see figure 1a [1], is called unconstrained. The sample is placed between two flat anvils during the test. This type has the advantage of a simple anvil design. The downside of this technique is the difficulty to accomplish a hydrostatic pressure throughout the specimen. When the pressure is applied, and the work piece is rotated, nothing obstructs the outward flow of



material at the edges. As a result, the diameter of the sample increases while in the center the backpressure due to friction is large, and no outward flow is possible. As a result, the thickness varies as function of the radius, with inhomogeneous properties as a result.

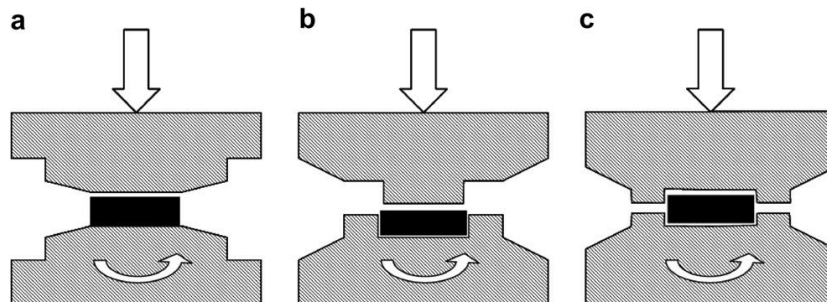


Figure 1: Unconstrained (a), constrained (b) and semi-constrained (c) HPT [1]

The second type is represented in figure 1b and is called constrained. The sample is placed within a mold which prevents outward flow completely. The hydrostatic pressure is constant throughout the specimen with more homogeneous properties after processing. The difficulty lies in the mold: designing the geometry and selection of appropriate materials is a difficult challenge. When the compression force is applied, both the specimen and the mold decrease in height. As a result, it is likely that the molds will come into contact and introduce high friction forces and wear rates in the contact surface. A compromise is found when using the quasi-constrained geometry represented in figure 1c. The outward flow is partially prohibited by placing the specimen in depressions in the anvils. However, the height of the specimen is larger than the depth of the depressions. This will result in large friction forces at the edges, ensuring hydrostatic pressure in the specimen, and lower wear rates in the anvils. This is the kind of HPT found in most literature and discussed here.

The grain refinement and the corresponding enhancement of mechanical properties obtained by a HPT process are to a large extent dependent on the pressure and strain imposed to the material. The distribution of the strain and the pressure in a sample is determined by the geometry and material of both the molds and the sample, and the friction between molds and sample. Numerical simulations have been used to study the conditions of the HPT process. In [2], the 3D deformation behaviour of a high density polyethylene sample during an unconstrained high pressure torsion process is simulated using the commercial Finite Element (FE) code MSC.Marc. The upper and lower anvils are assumed to be rigid bodies. A vertical displacement is imposed to the upper anvil in the compressive direction, and is maintained during torsion. In [3], the DEFORM FE software is used to perform isothermal simulations of unconstrained HPT for pure copper. Again, the anvils are modelled as rigid bodies, and are assumed to be tied to the deforming sample. This is also the case in [4,5] reporting isothermal FE simulations of unconstrained HPT for pure copper using Abaqus.

In this paper, the implicit, commercial FE code Abaqus/standard is used to simulate HPT processes. As opposed to most studies in literature [2-5], the real elasto-plastic behavior of the holders is modeled. Aiming at an in-depth understanding of the HPT process, the distribution and evolution of stresses and strains in the sample are simulated. Special attention is paid to the interaction between the mold deformation and the specimen behaviour.

2. Finite element model

For the finite element analyses, a disk shaped specimen with diameter $D = 10$ mm and thickness $H = 1.0$ mm is used. Semi-constrained conditions are adopted. A detail of the geometry of the upper part of the mold containing the cavity is shown in figure 2. The geometry is based on the molds used by CEIT (San Sebastian, Spain). In the finite element

model only the lower mold and half of the specimen -along the thickness direction- is modeled, using an appropriate symmetry boundary condition.

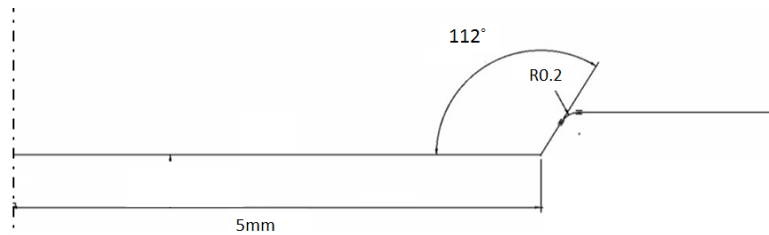


Figure 2: Geometry and dimensions of an axisymmetric section of the upper part, containing the sample cavity, of the mold

For both the sample and the mold, a classical metal, elasto-plasticity model with isotropic hardening is used. The sample is modelled as soft steel, with a Young's modulus $E = 210$ GPa and a Poisson coefficient $\nu=0.3$, the elasto-plastic properties are defined by a yield stress $\sigma_y = 100$ MPa, and a piecewise linear hardening curve that allows for severe plastic deformation (up to 500% strain at a stress of 760 MPa). Steel molds with different properties are considered. For the reference mold an initial yield stress of 1000MPa is considered and a linear small-slope hardening upto 4% of plastic strain. Additionally, simulations are performed with a yield stress level varying in the range of [500MPa;2500MPa].

Coulomb frictional contact conditions are applied at the interface between the steel sample and the mold. A friction coefficient of $\mu=0.4$ is used at the bottom of the cavity in the mold, 0.2 at the inclined edge. The axisymmetric section of the sample is meshed with 6600 CGAX4 elements. The CGAX4 element is a four node bilinear axisymmetric quadrilateral element allowing rotation. It is useful for the analysis of structures that are axially symmetric, but can twist about their symmetric axis, as is the case in high pressure torsion processes. To anticipate to the large deformations in the hoop direction during torsion, the elements are brickshaped with the smallest dimension along the thickness. For the steel mold 7967 CGAX4 elements are used.

To simulate compressive loading of the sample, a vertical displacement of 0.2mm is imposed to the lower part of the mould. In a second torsion step, a rotation of 0.75, corresponding with a rotation of nearly 86° for the full specimen, is applied, while maintaining the vertical displacement.

3. Results

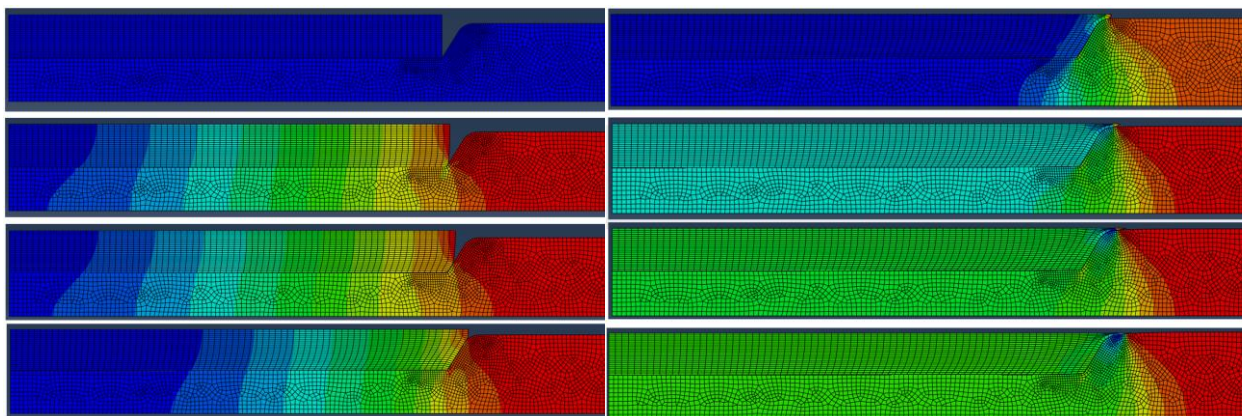


Figure 3: Subsequent stages of deformation of a HPT sample during the compression stage

Figure 3 represents subsequent stages of the sample deformation during compression. When the deformation is imposed, gradually the outside boundary of the sample comes in contact with the inclined edge of the cavity. Once the cavity is completely filled, sample material

starts to flow outwardly and the applied load is partially transferred from mold to mold by this material. During compression the thickness of the sample decreases. The thickness reduction is the highest at the outside border. During torsion the outward flow of the material continues and further thinning of the sample occurs.

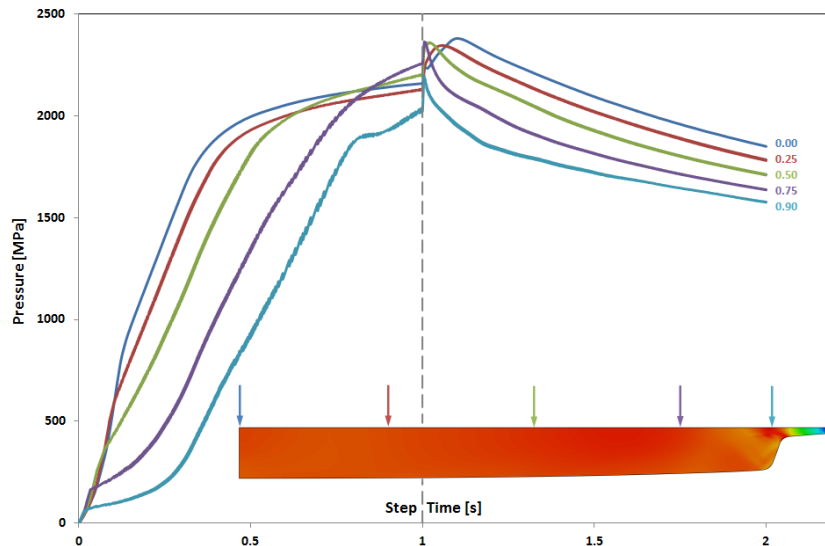


Figure 4: Evolution of the compressive stress at different locations in the sample during compression ($t < 1s$) and torsion ($t > 1s$)

In figure 4 the evolution of the axial pressure at different locations in the sample is given for the reference mold (initial yield strength of 1000MPa). The stress is clearly heterogeneous: except for a short period at the beginning, the stress is significantly higher close to the center of the sample. At higher levels of deformation in the compression stage, in the stress curves a sudden change in slope is observed which is caused by plastic deformation of the mold. Indeed, plastic deformation of the mold first occurs at the edge of the bottom of the cavity. Upon further deformation, at a certain distance beneath the center of the sample a rapidly growing region of plastically deformed mold material arises. In figure 5 the sample and a part of the die are represented at the end of the compression stage; the zones with a color different from deep blue are plastically deformed. The plastically deformed region in the die is responsible for the change in slope in the stress curves. As a result, the stress in the sample material above the plastically deformed mold material tends to saturate, which gives rise to more homogeneous stresses in the sample.

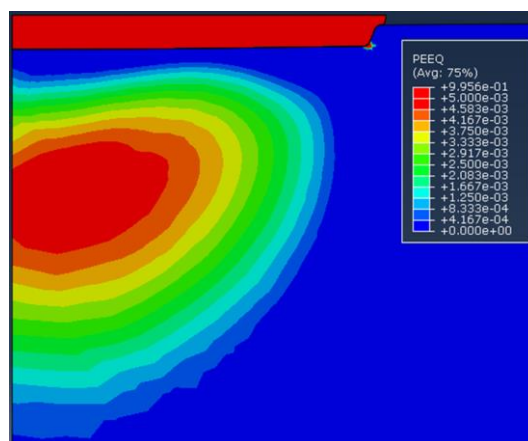


Figure 5: Contour plot of the plastic equivalent strain in the sample and a part of the mold at the end of the compression stage. The zones in dark blue have no or a negligible plastic deformation ($< 0.04\%$).

The effect of the molds' deformability on the pressure in the sample is clear from figure 6 which represents the pressure evolution in the centre and at $\frac{3}{4}$ of the sample radius away from the centre for a deformable and a rigid mold. The abrupt decrease in the slope of the curves observed for the deformable mold does not occur when a rigid mold is considered. As a result, for the latter, the stress inhomogeneity increases continuously. Since the change in slope is clearly related to plastic deformation of the mold, the yield strength of the mold affects the value at which the stress in the sample saturates. When a mold yield strength of 500MPa is considered the saturation value is close to 1100MPa; for a yield strength of 2000MPa sample stresses saturate at almost 3500MPa.

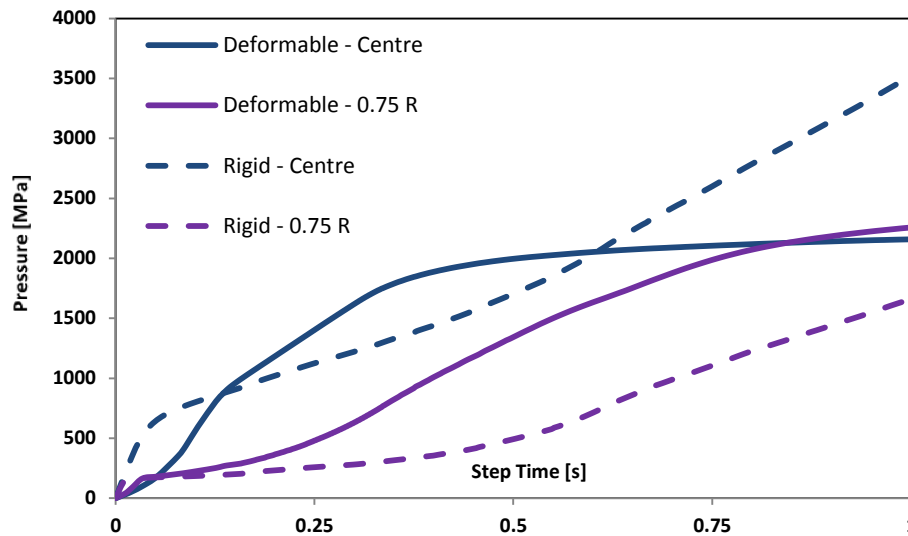


Figure 6: Evolution of the pressure in the centre and $\frac{3}{4}$ of the radius away from the centre for a deformable (full line) and rigid (dotted line) mold.

From time $t=1s$, the torsion deformation is imposed while maintaining the displacement imposed at the end of the compression step. Apart from the oscillations at the start of the rotation, the compressive stresses decrease and become more homogeneous.

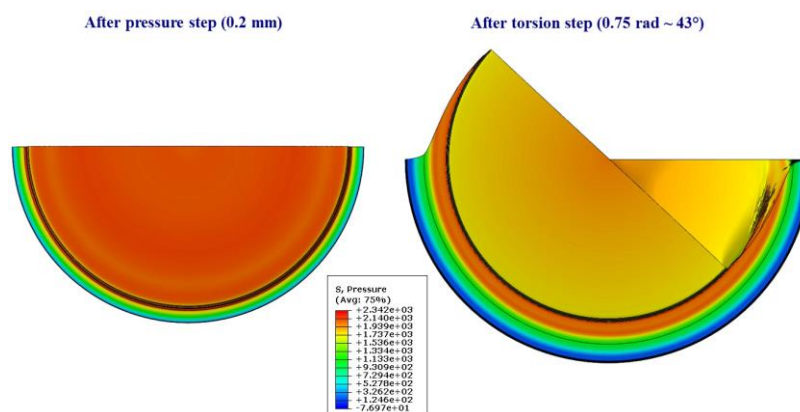


Figure 7: Deformed sample at the end of the compression (left) and torsion stage (right). The color code refers to the axial stress.

One quarter of the sample, seen from the top, at the end of the compression and torsion stage is represented in figure 7. The figure indeed shows that the outward flow of material continues during the torsion stage, resulting in a further decrease in thickness of the sample and a decrease of the stress. For the rigid mold model, the thickness reduction is constant. However, as can be seen in the inserted image of the deformed specimen in figure 4, the thickness reduction is more pronounced close to the outside border for a deformable mold.

4. Conclusions

In this contribution, results of finite element simulations of HPT processing are presented. As opposed to similar studies in literature, the real elasto-plastic behavior of the holders is modeled. Attention is focused on the distribution of compressive stress and deformation in the material sample. The simulations show that from a certain level, due to plastic deformation in the sample holders, increasing the applied force no longer results in a proportional increase of the stress in the sample. Indeed, the pressure in the sample tends to saturate to a value related to the yield strength of the holders. Again as a result of the deformability of the holders, also the sample deformation is highly heterogeneous with significantly higher thickness reductions at the outside border. Major conclusion is that the real deformation properties of the mold material should be taken into account when HPT processes are modelled.

Acknowledgement

The authors would like to acknowledge the IUAP program of the Federal Science Policy of Belgium and the partners of IUAP-VII-project P7/21 'Multiscale mechanics of interface dominated materials'.

References

- [1] Zhilyaev AP and Langdon TG 2008 Using High Pressure Torsion for Metal Processing: Fundamentals and Applications. *Progr. Mat. Sci.* **53**:893-979.
- [2] Draï A and Aour B 2013 Analysis of Plastic Deformation Behavior of HDPE during High Pressure Torsion Process. *Eng. Struc.* **46**:87-93.
- [3] Yoon SC, Horita Z and Kim HS 2008 Finite Element Analysis of Plastic Deformation Behaviour during High Pressure Torsion Processing. *J. Mat. Proc. Tech.* **201**:32-36.
- [4] Kim HS 2001 Finite Element Analysis of High Pressure Torsion Processing. *J. Mat. Proc. Tech.* **113**:617-632.
- [5] Kim HS, Hong SI, Lee YS, Dubravina AA and Alexandrov IV 2003 Deformation Behavior of Copper during High Pressure Torsion Processing. *J. Mat. Proc. Tech.* **142**:334-337.